GBT Commissioning Memo 11:
Plate Scale and pointing effects of subreflector positioning at 2 GHz.

Keywords: low frequency Gregorian, plate scale, focus tracking, pointing.

N. VanWey, F. Ghigo, R. Maddalena, D. Balser, G. Langston, M. McKinnon
July 18, 2001

Summary

We have considered pointing offsets that result from motion of the Gregorian subreflector along its X and Y axes. The only expected offset is that the elevation changes with motions in the X axis, which can be characterized by a linear "plate scale". We have found evidence that this relation is not linear. We have also found evidence that the X and Y motions of the subreflector are not along the ideal Xs and Ys axes, but are tilted by small amounts of the order of a degree.

A. Introduction

In this memo, we will consider what pointing offsets might be caused by motions of the subreflector. This memo uses the same data referred to in GBT Commissioning memo 7 "Gregorian Focus Tracking at S-band" (March 29, 2001). Refer to that memo for details of the observing.

Figure 1 shows the subreflector geometry. The Y axis (Y_s in Fig.1) is towards and away from the primary (100-m) reflector; the X axis (X_s in Fig.1) is in the plane bisecting the feed arm and the primary reflector. The "Z" axis rises out of the paper perpendicular to X and Y. The (Xs, Ys, Zs) notation is used in GBT memo 165 (Goldman, Feb. 1997). In this paper we will simply use (X, Y, Z) for the subreflector axes.

Motions of the subreflector along the X axis produce changes in the elevation of the beam on the sky. The effect can be characterized by a "plate scale", i.e., the elevation offset corresponding to an offset of the subreflector in the X coordinate.

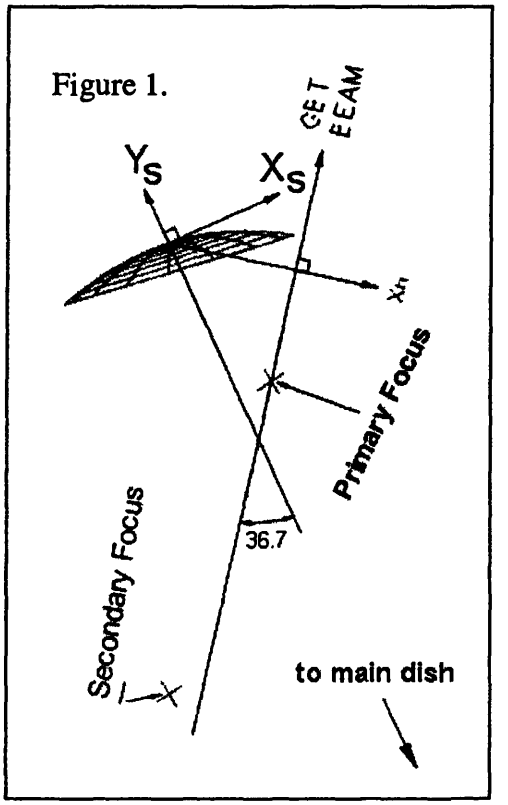

The measurement of the plate scale is described in section C. The effect of X motion of the subreflector on the azimuth pointing is not zero as expected and is described in section D. Motion of the subreflector in the Y direction should, by design, produce minimal pointing offsets. We discuss Y motion effects on elevation in section E, and effects on azimuth in section F.

B. Procedure

Measurements were made during February 23rd to March 6th of 2001 to determine the optimum X and Y focus settings as a function of elevation. Observing was at a frequency of 2.0 GHz with 80 MHz bandwidth in linear polarization. The noise calibration was switched at 2 Hz rate. Total power detection was in the IF rack, and data was recorded with the DCR. The observing procedure was the same as described in GBT commissioning memo 7. A summary of observations may be found in Tables 1 and 2 of memo 7.

Many focus scan sequences were done, moving the subreflector in X (X-sequence) and in Y (Y-sequence). A focus scan sequence consisted of stepping the focus through its range. At each step a calibration source was observed using a "cross" or "crossupdate" procedure to find the peak amplitude of the observed radio source and its pointing offset.

The steps in Y were from -10 inches to +10 inches (-254 to +254 mm) by steps of either 2.0 or 2.5 inches (51 or 64 mm). For X the steps went from -9 to +9 inches (-228.6 to +228.6 mm), also by steps of 2.0 or 2.5 inches.

A "cross" or "crossupdate" procedure consists of 4 scans: a scan across the source first in increasing RA, then back, followed by a scan in increasing DEC, then back. After each set of scans, new LPCs were calculated giving the improved pointing offsets. These corrections were determined by the on-line program "GO_point" by fitting a gaussian curve to each scan. The center position of each fitted gaussian gives the position offset from the LPCs. These offsets were added to the LPCs to give a total position correction (delta-az, and delta-el), i.e., the correction to the telescope encoder settings. Thus we acquired a data set giving the position corrections (delta-az and delta-el) for a variety of X and Y subreflector settings and telescope elevations.

The data set we used consisted of the pointing cross data taken as part of sequences in X or Y, not data taken during these days for other purposes. We also eliminated several scans that were contaminated by RFI.

C. Elevation errors as a function of X .

To illustrate the change in elevation pointing with the X position, we show d (EL) plotted versus X in Figure 2, for three different elevations. The relation is linear for each X sequence, with similar slope. This illustrates the "plate scale" in X. The offset between the three lines is due to the elevation dependant effects, i.e., the gravitational deflection of the feed arm and the main reflector. Note that the slope differs significantly for the low elevation data (El=10°).

The whole data set is plotted in Figure 3. For each X, the curve of d(EL) versus elevation is plotted. Each curve is the pointing error as a function of elevation when the subreflector X is fixed. The rise at low elevation is due to atmospheric refraction, which can be modeled to sufficient accuracy as a term in cotangent of the elevation. A model was fit to the data set of the form:

$$d(EL) = A0 + A1*X + A2*\cot(EL) + A3*\cos(EL) + A4*\sin(EL)$$

In Figure 3, the fitted model is plotted as the solid curves. The residuals to the fit are shown in Figure 4. The parameters of the model fit are listed in Table 1, and the rms of the residuals is about 8.9 arcsec. The best estimate of the plate scale is the parameter A1, which worked out to -3.624"/mm.

Figure 2.

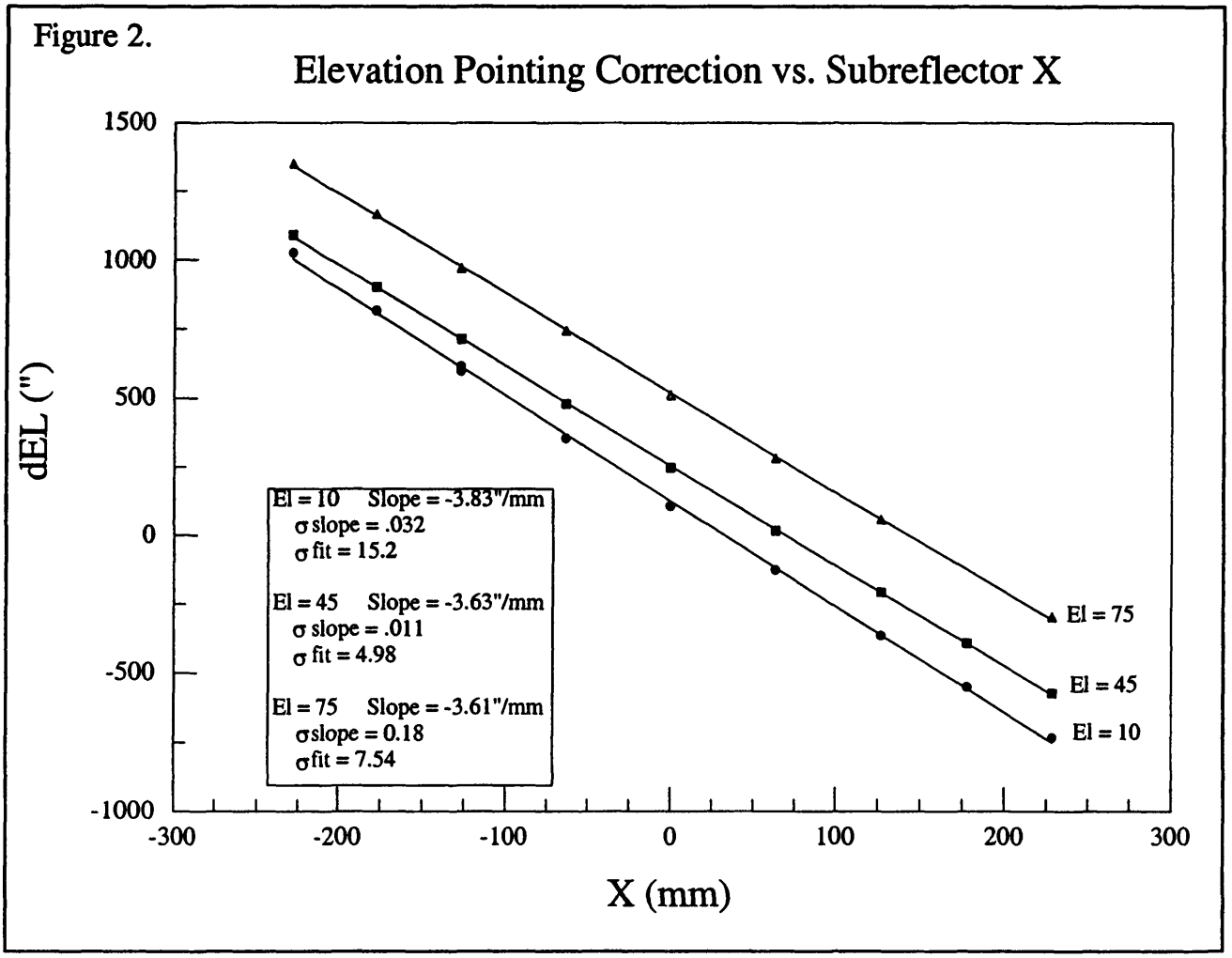

Table 1. Model fit to elevation pointing correction as a function of X and Elevation.

Parameter	Value	Term
A0	107.8" (22)	1
A1	-3.624"/mm (.0036)	X
A2	53.7" (1.6)	cot(EL)
A3	-382.9 " (12)	cos(EL)
A4	500.6" (18)	sin(EL)
rms residual	8.9"	

Figure 3.

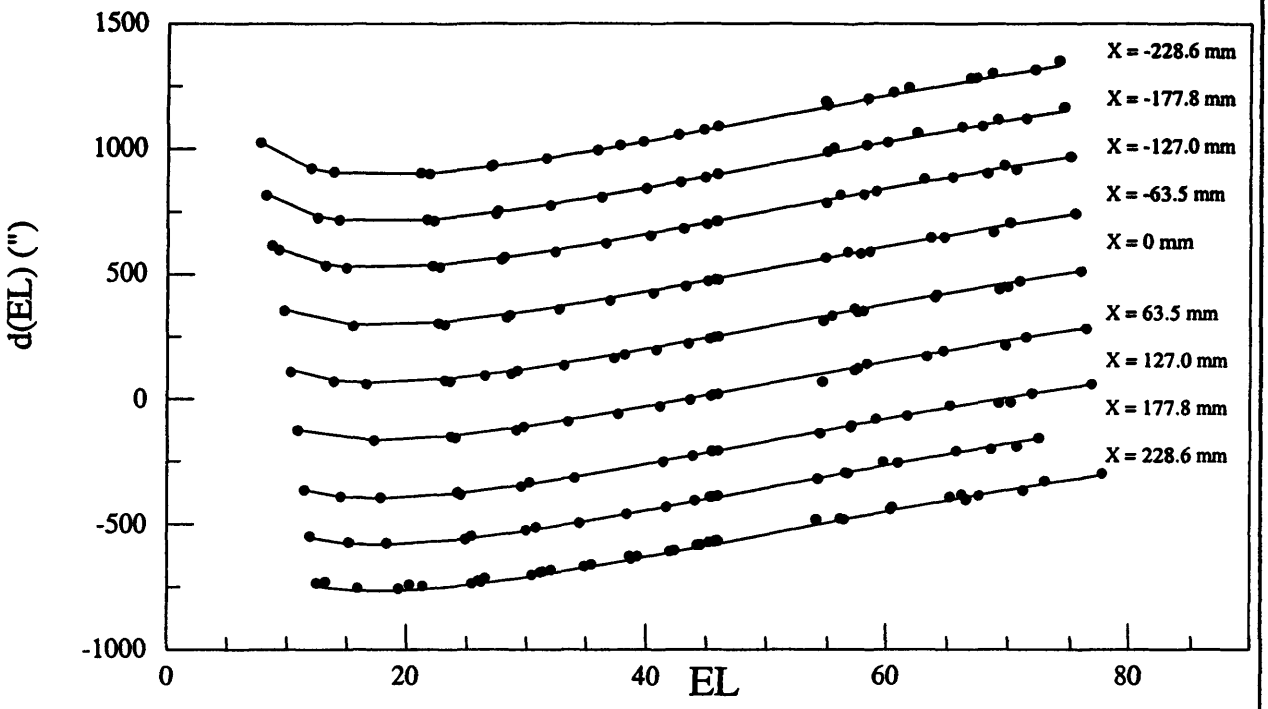

fit to d(EL) = 107.8 + 53.66 COT(EL) -382.93 COS(EL) + 500.6 SIN(EL) - 3.624 * X

Figure 4.

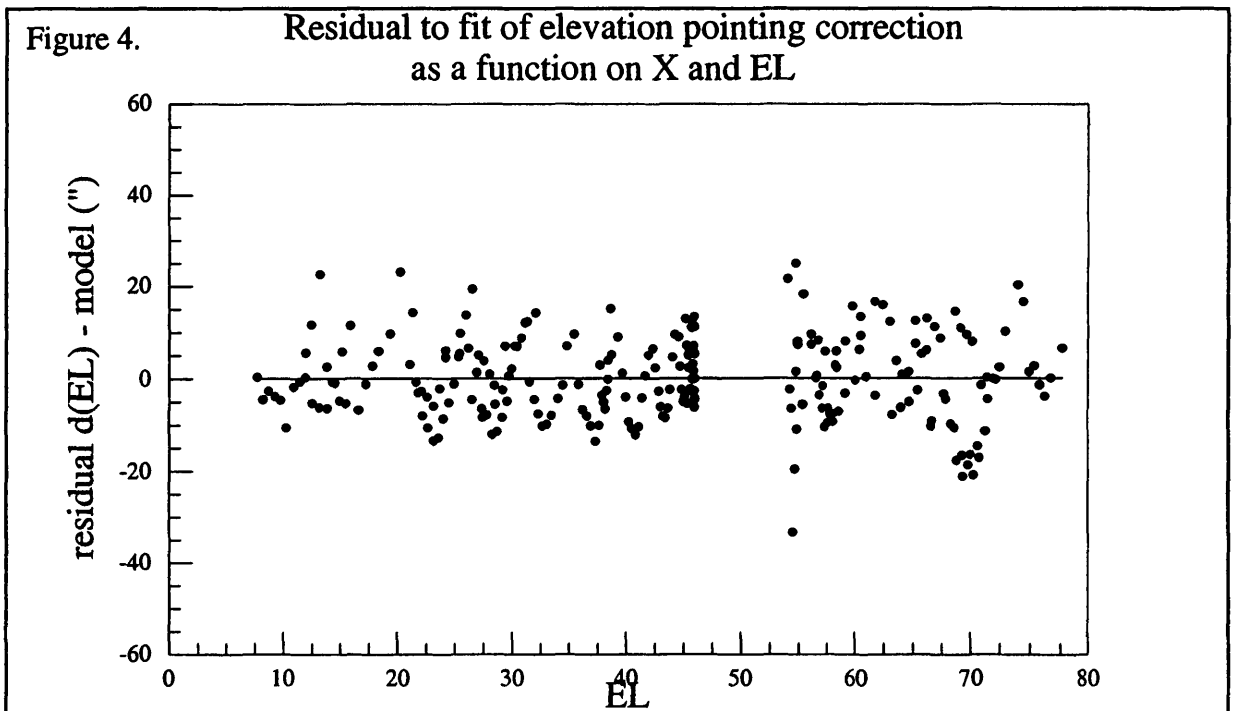

residual = d(EL) - (107.8 + 53.66 *COT(EL) - 382.93 *COS(EL) + 500.6*SIN(EL) - 3.624*X)

model σfit = 8.9

One may note, in Figure 4, that there seems to be some structure in the plot of residuals. This becomes clear when the residuals are plotted versus X, as shown in Figure 5. Thus after removing the elevation dependence (i.e., the pointing equation), and a linear plate scale, there remains a non-linear relation between elevation error and X. A fourth-order polynomial was fit the data and is shown in Figure 5 as the solid curve.

The non-linear effect may be due to a non-planar focal surface, or could result from an improper transformation between the actuator motions and the subreflector (Xs, Ys, Zs) coordinate system.

Figure 5.

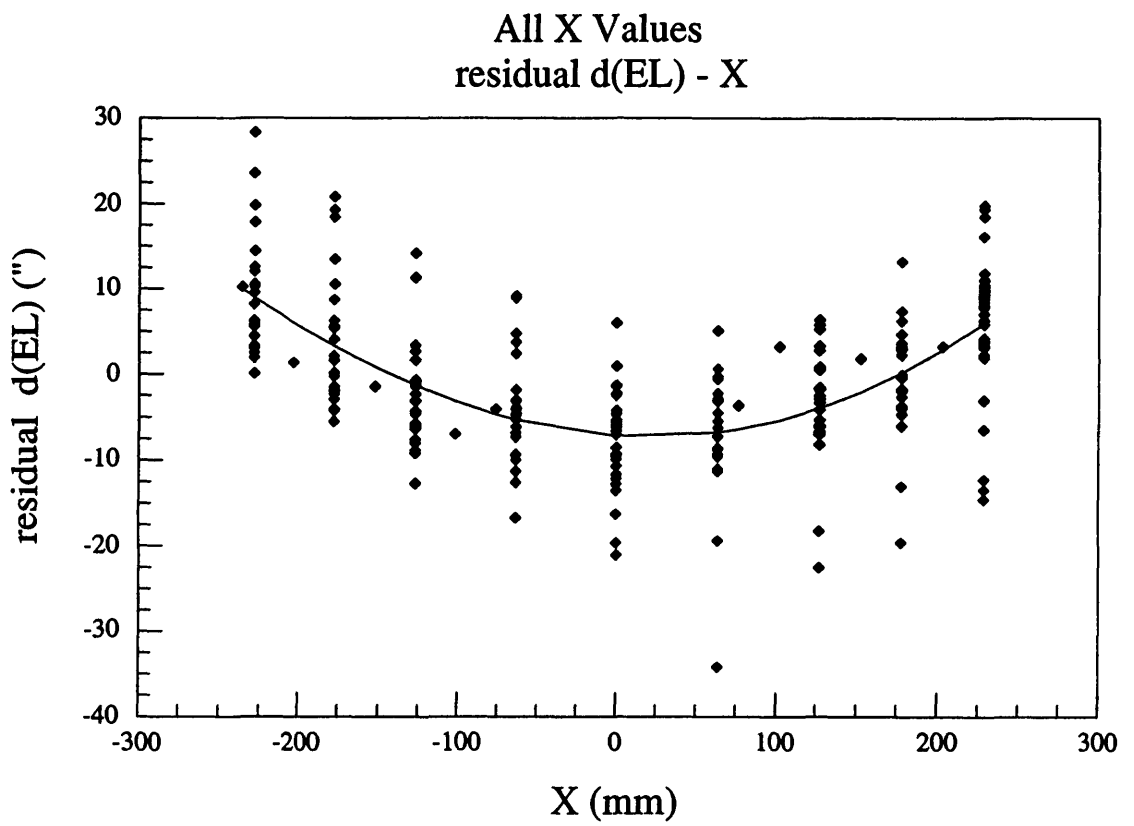

To see what, if any, relation the elevation might have on these results, we have plotted in Figure 6 a similar diagram of elevation residuals vs. X for 4 different ranges of elevation. The same polynomial that was fit to the full data set is plotted as the solid line on each graph in Figure 6. One can see that the rms scatter about such a fit varies considerably for the different elevation ranges. For elevations between 0 and 32° and 32°-46°, the rms deviation is about half that for the higher elevations. The significance of this is not at all clear at the moment.

Note that the rms deviations from the solid curves are summarized in Table 5, at the end of the paper. The column labeled "X-d(EL)" in Table 5 summarizes the results for the data plotted in Figures 5 and 6.

Figure 6. Elevation residuals versus X for different elevation ranges.

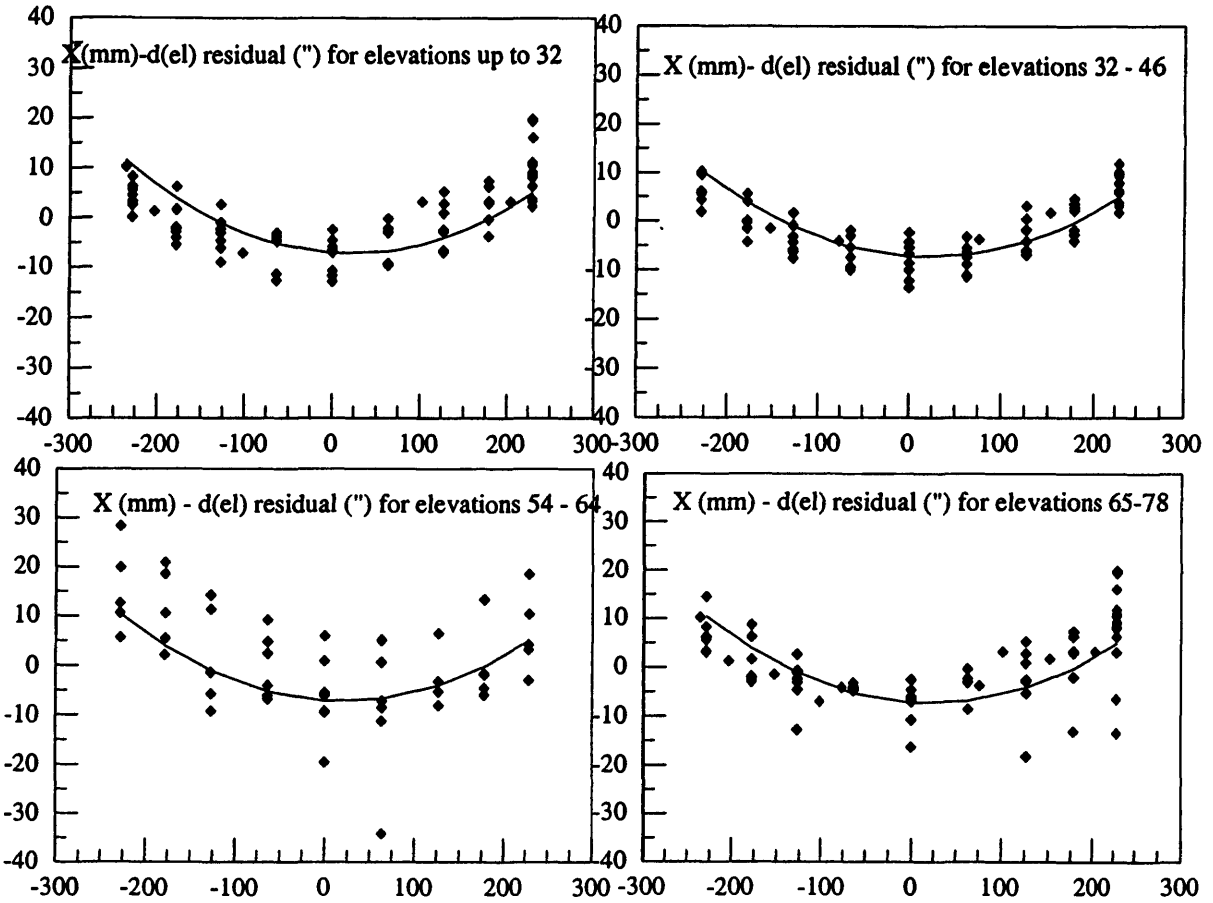

The non-linear plate scale seems to be mostly independent of elevation. But the points in the upper right plot of Figure 6 (elevation < 32°) do not fit the curve as well as the others. There may be small elevation dependent effects.

D. Azimuth errors as a function of X.

The azimuth pointing corrections are plotted in Figure 7 as a function of elevation. The different X settings are plotted as different symbols. One notes that there is a small but systematic difference between the various X settings. A model similar to that described for the elevation corrections was fit to this data set, with the results listed in Table 2. The solid curves in Figure 7 are the model for the different values of X.

Table 2. Model to fit azimuth pointing correction as a function of X and Elevation.

Parameter	Value	Term
A0	-128.3" (8.0)	1
A1	-0.0327"/mm (0.0024)	X
A2	490.67" (6.4)	cos(EL)
A3	91.2" (5.5)	sin(EL)
rms residual	5.4"	

One notes that the azimuth plate scale (A1) is small (-0.033"/mm), but significant. Moving the subreflector over its full X range of 500 mm results in a shift of 17".

Figure 7.

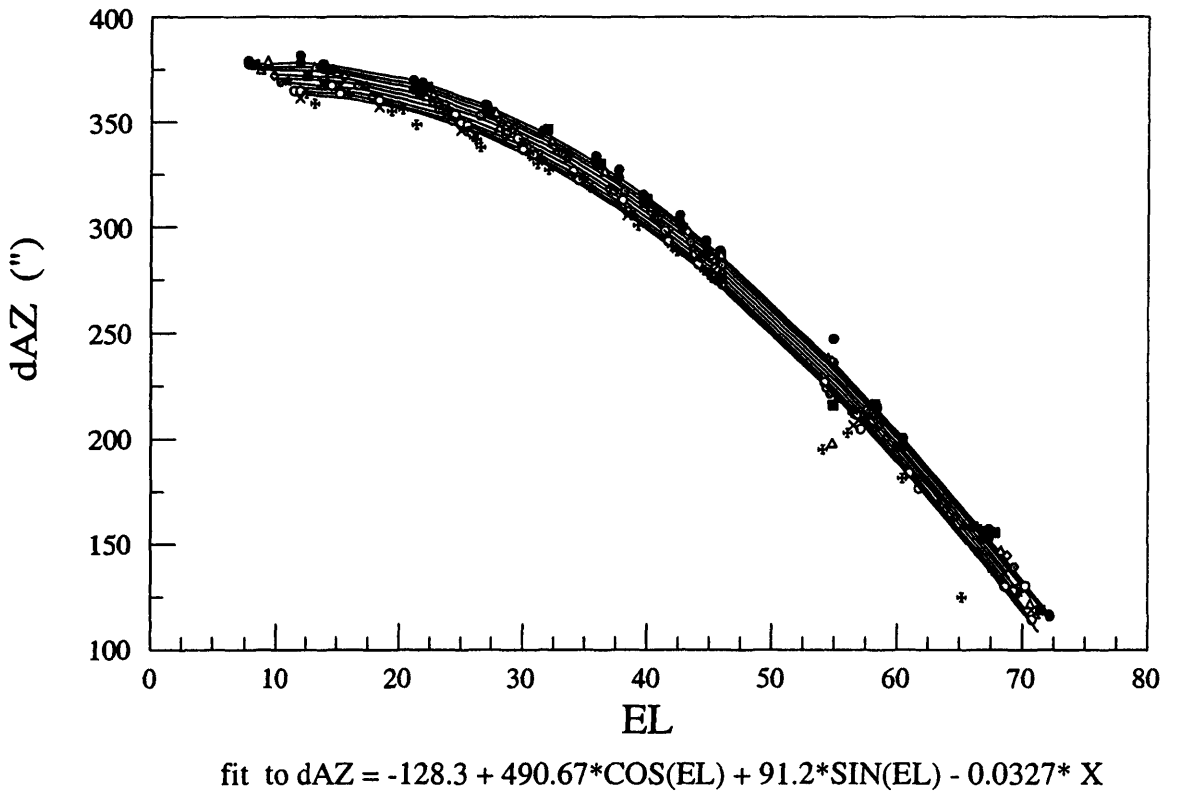

A model was fit to the data set in which the linear term in X was not used. The resulting model is

$$dAZ = -118.6 + 482.8\cos(EL) + 84.0\sin(EL).$$

The residuals to this second model are plotted versus X in Figure 8, showing the remaining linear trend.

Figure 8.

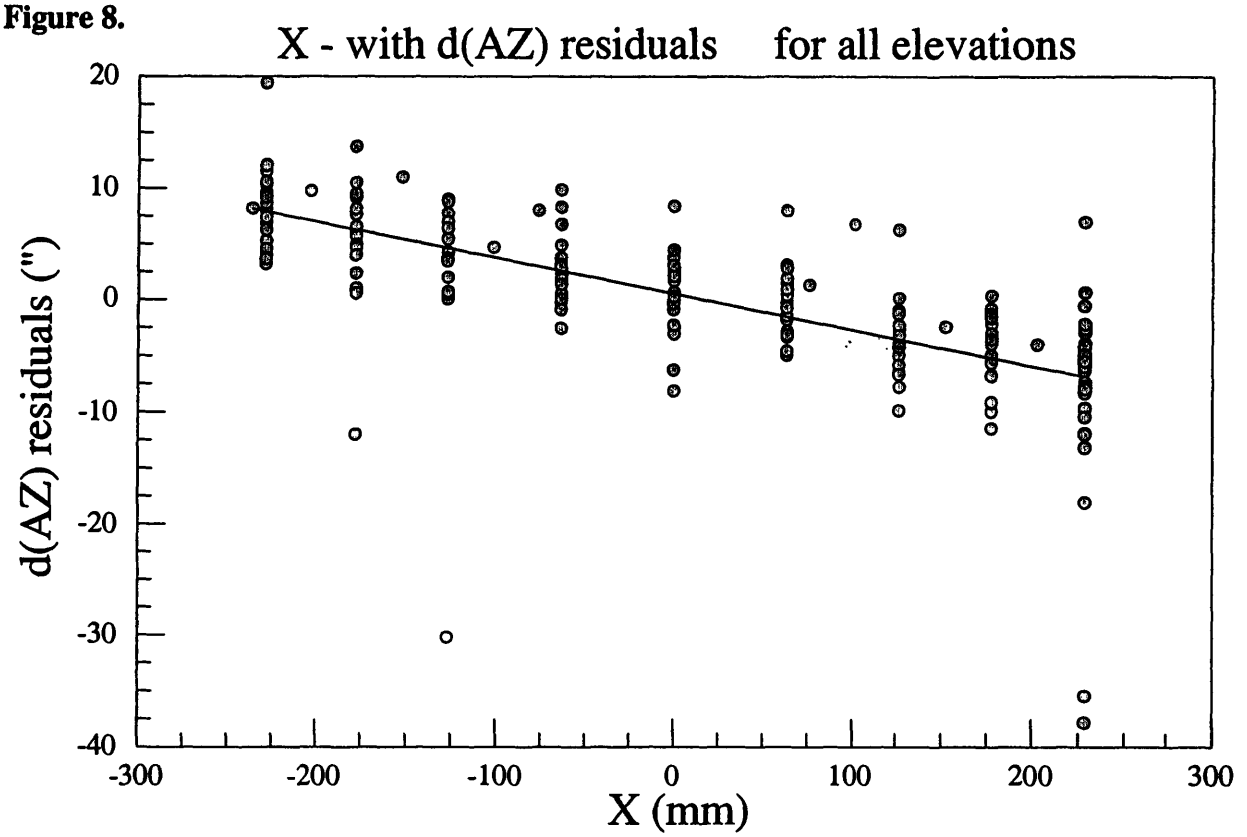

Again, we have divided the data into subsets for different elevation ranges. The residual plots for these subsets are shown in Figure 9, and the rms deviations from a straight line fit to the full data set are listed in Table 5. Again we find the scatter is less at the lower elevations (elevation < 46°).

A likely explanation for the linear trend is that the "X-axis" along which the subreflector is moving is not the designed Xs axis, but is tilted a little. The amount of skew can be estimated from

$$\theta = \tan^{-1}(0.0327 / 3.63) = 0.52°$$

Thus it appears that the axis along which the subreflector is actually moving is titled in the Z direction by about half a degree from the ideal X axis.

Figure 9.

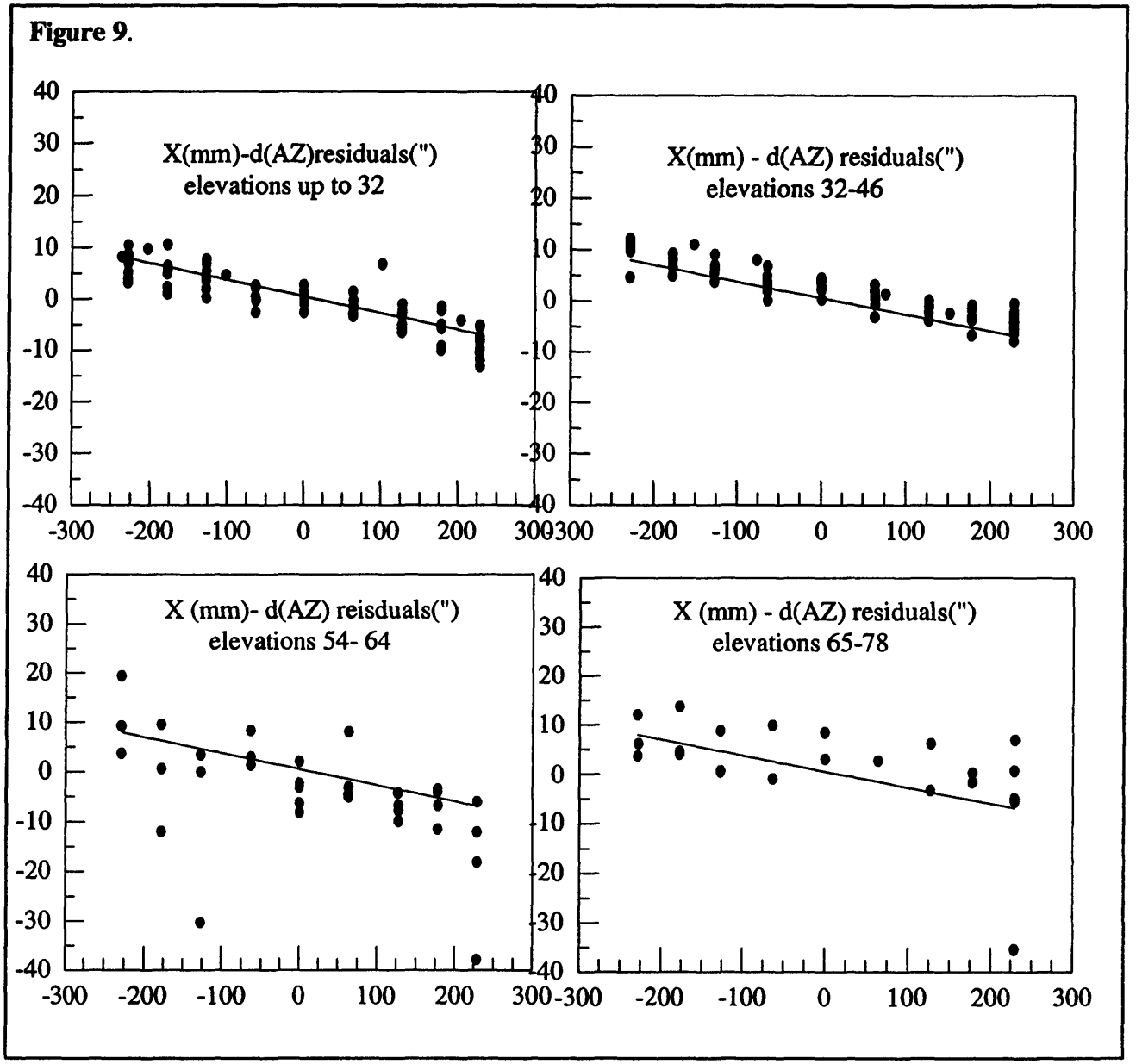

The tilt is mostly independent of elevation, although there may be a small difference in the highest elevation plot (65-78°).

E. Elevation pointing corrections as a function of Y.

Next we consider the data set in which pointing offsets were determined for several sequences of moving the subreflector along the Y axis. For some of these sequences the X coordinate was set to some value other than zero. In these cases the elevation offsets were corrected for the X position using the linear plate scale derived in section C.

The elevation pointing corrections are plotted in Figure 10 as a function of the elevation. The elevation pointing corrections are shifted based on the X value using the equation

$$d(EL)\text{shifted} = d(EL) + 3.634 * X$$

The different Y settings are plotted as different symbols. There is a small but systematic difference between the different Y settings. The model was fit to these elevation errors similar to that used for the X-sequence data:

$$D(EL) = A0 + A1*Y + A2*\cot(EL) + A3*\cos(EL) + A4*\sin(EL)$$

The fitted parameters are listed in Table 3.

Figure 10

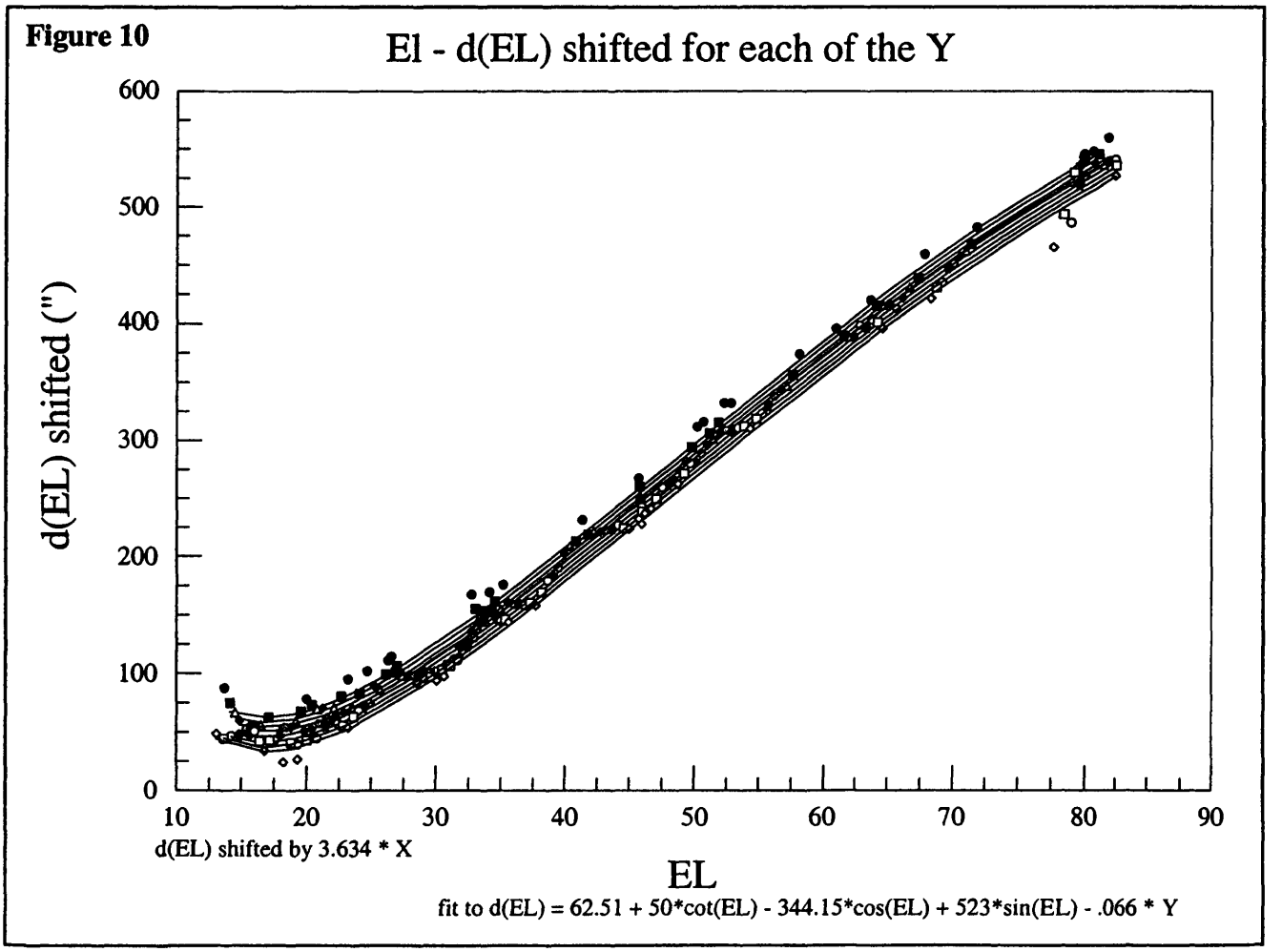

Table 3. Model to fit elevation pointing corrections as a function of Y and Elevation

Parameter	Value	Term
A0	62.51" (21)	1
A1	-0.0665"/mm (0.0033)	Y
A2	50.0" (2.7)	cot(EL)
A3	-344.1" (8.8)	cos(EL)
A4	523.1" (19)	sin(EL)
rms residual	8.2"	

The sinusoidal pattern seen in the data points in Figure 10 (also in Figure 7) is an artifact of the order of taking data. The Y value was changed from –254mm to +254mm and back repeatedly, producing related changes in d(EL). The effect is seen in a magnified view, Figure 11, in which the elevation dependent terms have been subtracted out.

Figure 11.

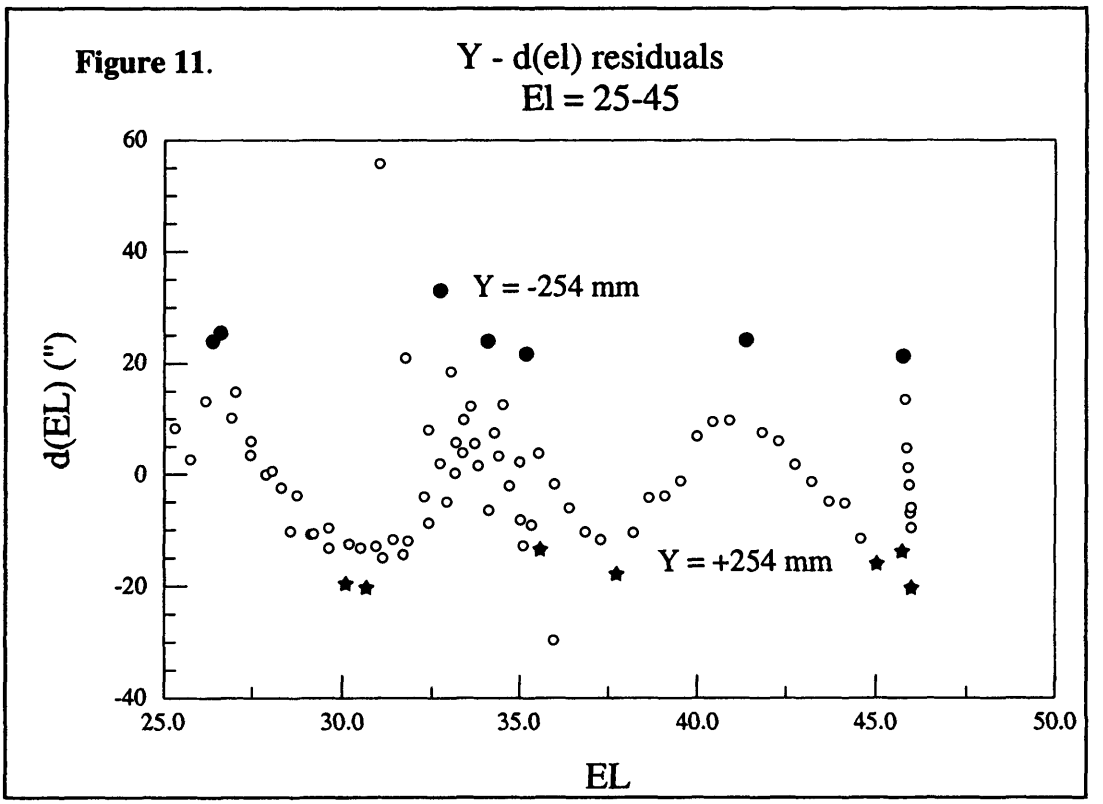

The effect is more clearly seen in a plot of the elevation residuals versus Y, shown below in Figure 12. Here the elevation dependent terms have been subtracted out, but the linear term in Y has not. From the fit results in Table 3, the slope of the line in Figure 12 is –0.0665"/mm.

The plot of the d(El) residuals as a function of Y for all points is shown below in Figure 12, and the same data, separated into different elevations is in Figure 13. The rms values with respect to a linear fit for these are in Table 5.

Figure 12.

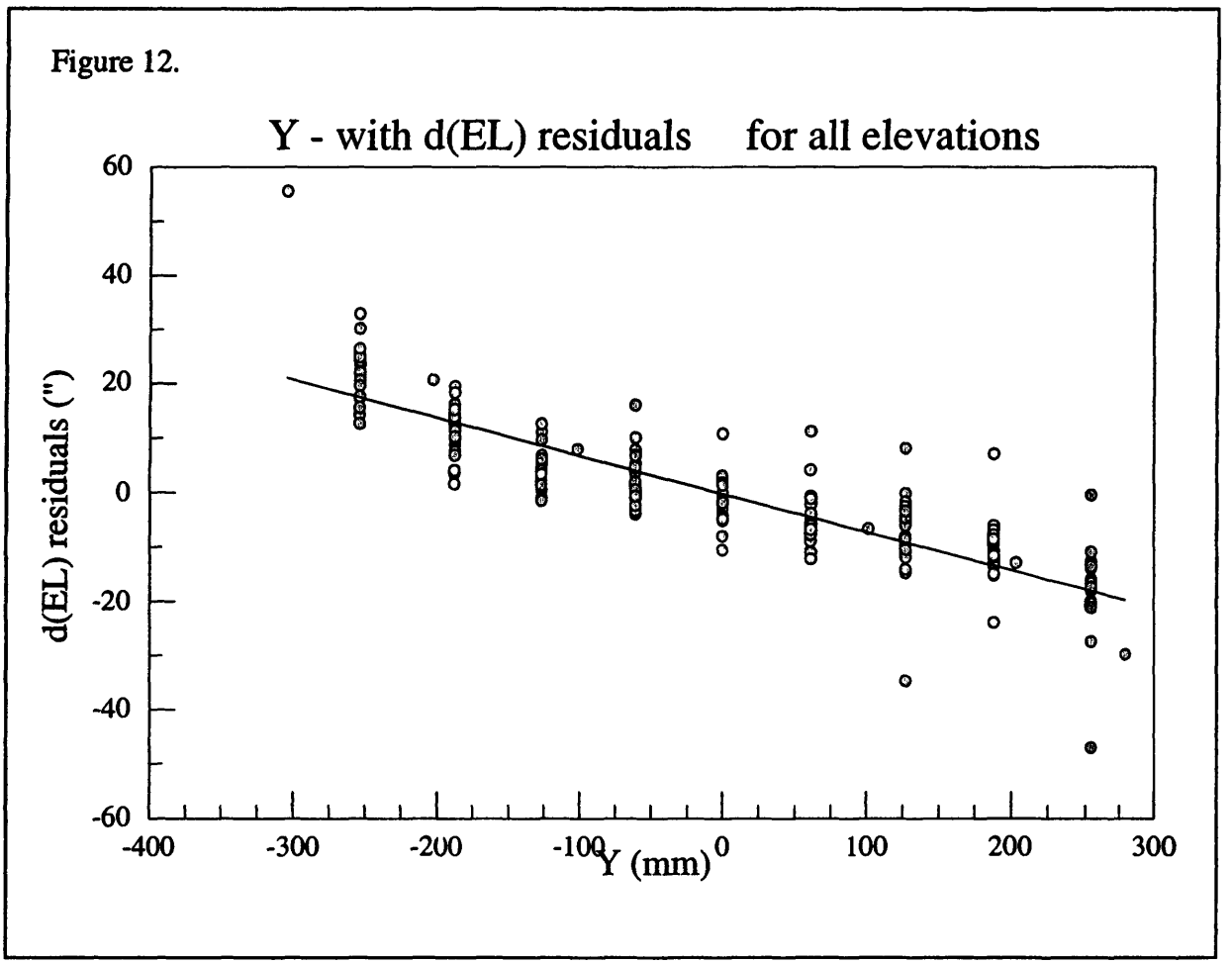

Figure 13.

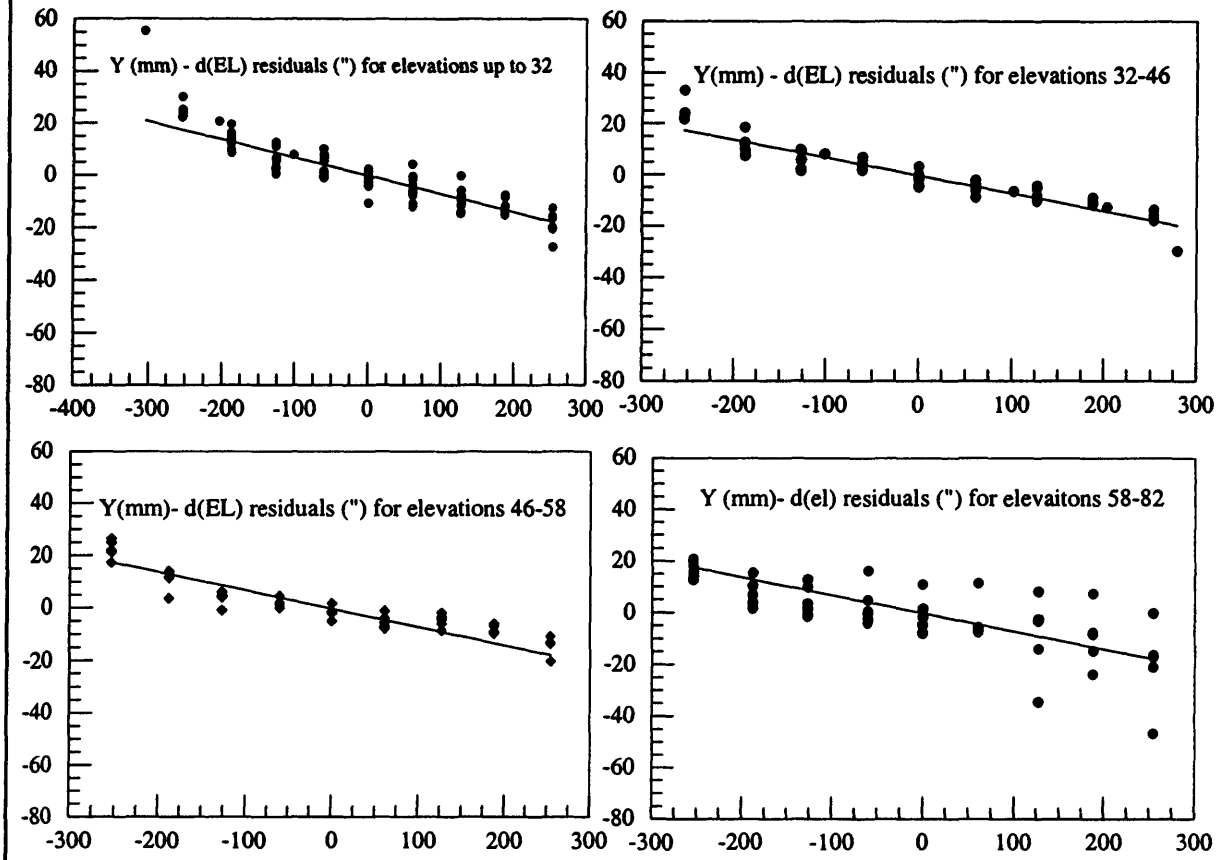

If we consider the average linear term to result from a skew of the Y travel of the subreflector from the ideal Y-axis, then we can derive the angle:

$\theta = \tan^{-1}(0.0665/3.634) = 1.05°$

Thus it appears that the Y travel of the subreflector is tilted in the X direction by about 1°.

F. Azimuth corrections as a function of Y

The azimuth pointing corrections as a function of the elevation at each of the Y settings are plotted in Figure 14. The different Y settings are marked with different symbols. The lines for each of the 9 different Y settings are plotted separately, and are essentially equivalent, indicating no change in the azimuth corrections as a function of the Y value. The lines are fit to:

$$d(AZ) = A0 + A1*\cos(EL) + A2*\sin(EL)$$

with the results listed in Table 4.

Table 4. Model to fit azimuth pointing correction as a function of elevation

Parameter	Value	Term
A0	-143" (5.1)	1
A1	507.6" (3.8)	cos(EL)
A2	99.8" (4.0)	sin(EL)
rms	4.5"	

Figure 14.

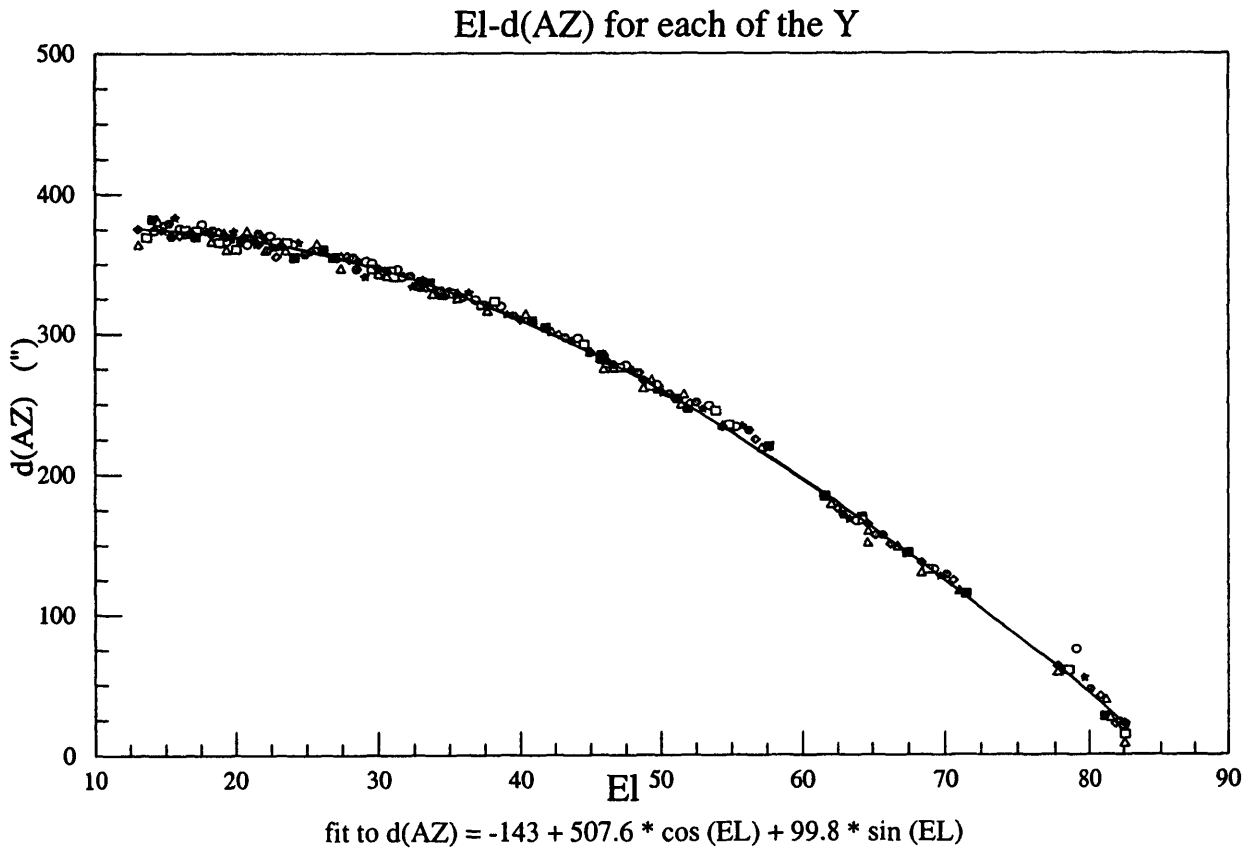

The graphs of the d(AZ) residuals as a function of Y are shown in Figure 15 for all points and in Figure 16 for the separate elevations. In all cases, these are residuals to the model listed in Table 4.

Figure 15.

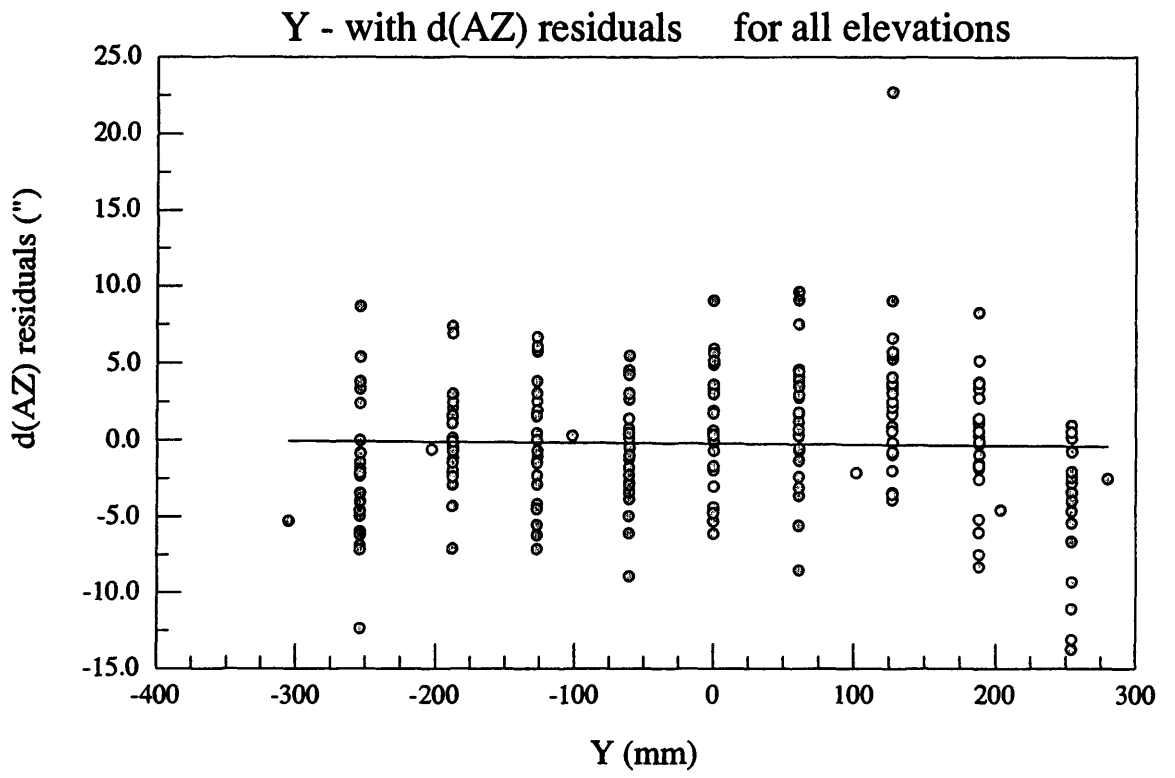

Figure 16.

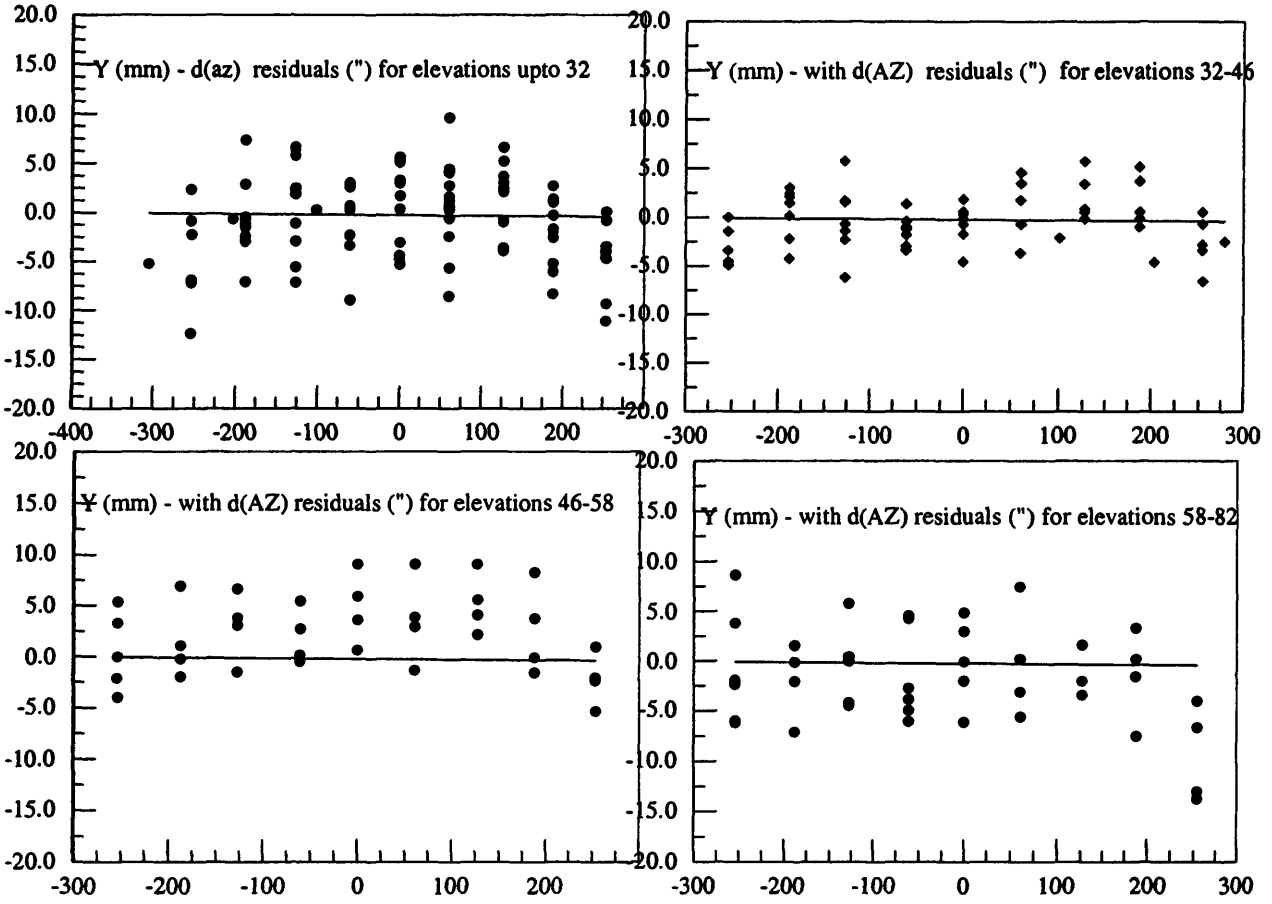

We see little sign of tilting of the Y axis in the Z direction from the residuals plotted in Figure 15. The plots in Figure 16, for different ranges in elevation show possible non-linear effects which should be investigated further.

Finally, Table 5 summarizes the residuals to the various models, both for the whole elevation range (the "All" row) and for the 4 different subsets.
The "X-d(AZ)" column summarizes rms deviations illustrated in Figures 8 and 9; "X-d(EL)" corresponds to Figures 5 and 6; "Y-d(AZ)" to Figures 15 and 16; and "Y-d(EL)" to Figures 12 and 13.

Table 5. rms deviation of residuals to the various models.

Elevation	X-d(AZ)	X-d(EL)	Y-d(AZ)	Y-d(EL)
0-32	2.6"	4.0"	4.4"	5.7"
32-46	5.3"	3.1"	2.6"	3.1"
54-64	8.2"	8.3"	3.2"	2.7"
65-80	7.9"	9.4"	5.3"	8.7"
All	5.3"	6.9"	4.5"	6.3"

Conclusions

- The X-axis is tilted in Z by about 0.5°, and the effect may have a slight elevation dependence.
- The X-axis plate scale is non-linear, and should be compared with theoretical optical models. There may be a slight elevation dependence.
- The Y-axis is tilted in X by about 1.0°, and the effect does not appear to be elevation dependent.

The tilts imply that the actuator axes are not calibrated properly, or the subreflector mount is mis-set. The tilts can be corrected by recalibration of axes, or remounting the subreflector. Another possibility is to add terms to the focus tracking algorithm to correct these errors.

These results mean that the focus tracking model we have been using since mid March of 2001 is incorrect. The pointing model is compensating for these effects. The effects on gain or pointing will not become significant until we start observing at high frequencies of 80 GHz or more. We will need to address these problems for phase III commissioning.